


RESEARCH

Open Access



The comparative anti-cancer effects of krill oil and oxaliplatin in an orthotopic mouse model of colorectal cancer

Abilasha Gayani Jayathilake¹, Majid Hassanzadeganroudsari¹, Valentina Jovanovska¹, Rodney Brain Luwor², Kulmira Nurgali^{1,3,4*†} and Xiao Qun Su^{1*†} 

Abstract

Background: Our in vitro studies demonstrated that krill oil (KO) has anti-cancer potential. This study aimed to compare the anti-cancer effects of KO with a commonly used chemotherapeutic drug, oxaliplatin and to identify the molecular mechanisms associated with KO supplementation in a mouse model of colorectal cancer (CRC).

Methods: Thirty-six male Balb/c mice were randomly divided into six groups. Five groups received standard chow diet supplemented with KO (150 g/kg), corn oil (150 g/kg), KO combined with ½ dose of oxaliplatin (1.5 mg/kg body weight/3 times per week), corn oil combined with ½ dose of oxaliplatin (1.5 mg/kg body weight/3 times per week), or a full dose of oxaliplatin (3 mg/kg body weight/3 times per week). The control (sham) group received a standard chow diet. Treatments started three weeks before and continued for three weeks after orthotopic CRC induction. The number of metastases, tumour weight and volume were quantified *ex-vivo*. The expression of cytochrome *c*, cleaved caspase-9 and -3, DNA damage, PD-L1, PD-L2 and HSP-70 were determined.

Results: A significant reductions in the weight and volume of tumours were observed in mice treated with KO and KO plus a ½ dose of oxaliplatin compared to the sham group, similar to oxaliplatin-treated mice. KO, and KO plus ½ dose of oxaliplatin significantly increased the expression of cytochrome *c*, cleaved caspase-9 and -3, and DNA damage and decreased expression of PD-L1, PD-L2 and HSP-70 in tumour tissues compared to the sham group.

Conclusions: The in vivo anti-cancer effects of KO are comparable with oxaliplatin. Thus, dietary KO supplementation has a great potential as a therapeutic/adjunctive agent for CRC treatment.

Keywords: Krill oil, Oxaliplatin, Orthotopic model of colorectal cancer, Caspase 3/9, PD-L1/PD-L2, HSP-70

Background

Colorectal cancer (CRC) is the third most common cancer and the fourth leading cause of cancer-related mortality worldwide, with almost 1.8 million new cases and 881,000 deaths reported in 2018 [1]. A complete resection of the primary tumor would be effective to cure CRC

diagnosed at an earlier stage. However, CRC is often asymptomatic at an early stage, and most cases are identified at a late stage. Approximately 56% of patients die from CRC due to distant metastases present in approximately 25% of patients at the initial diagnosis [2–4]. Currently, the advanced stage of CRC is treated with chemotherapy, radiotherapy, their combination, or adjuvant pre- or post-surgical chemotherapy. Commonly used chemotherapeutic agents are 5-fluorouracil (5-FU), oxaliplatin, irinotecan, or their combinations. Unfortunately, these treatments associate with numerous acute

*Correspondence: kulmira.nurgali@vu.edu.au; xiao.su@vu.edu.au

†Kulmira Nurgali and Xiao Qun Su contributed equally

¹ Institute for Health and Sport, Victoria University, P.O. Box 14428, Melbourne 8001, Australia

Full list of author information is available at the end of the article



© The Author(s) 2022. **Open Access** This article is licensed under a Creative Commons Attribution 4.0 International License, which permits use, sharing, adaptation, distribution and reproduction in any medium or format, as long as you give appropriate credit to the original author(s) and the source, provide a link to the Creative Commons licence, and indicate if changes were made. The images or other third party material in this article are included in the article's Creative Commons licence, unless indicated otherwise in a credit line to the material. If material is not included in the article's Creative Commons licence and your intended use is not permitted by statutory regulation or exceeds the permitted use, you will need to obtain permission directly from the copyright holder. To view a copy of this licence, visit <http://creativecommons.org/licenses/by/4.0/>. The Creative Commons Public Domain Dedication waiver (<http://creativecommons.org/publicdomain/zero/1.0/>) applies to the data made available in this article, unless otherwise stated in a credit line to the data.

and long-term side effects. Nearly 85% of patients reduce the dose or discontinue the treatment due to these side effects [5].

Oxaliplatin is a third-generation platinum-based anti-cancer chemotherapeutic drug primarily used as a first-line treatment for metastatic colon or rectum cancer. The side effects associated with oxaliplatin treatment include peripheral neurotoxicity, nephrotoxicity, cardiotoxicity, and several gastrointestinal (GI) complications such as diarrhoea, nausea, abdominal pain, vomiting, and anorexia [6]. The symptoms can continue for up to 10 years after treatment has stopped [7, 8].

Epidemiological and experimental findings have shown that natural products containing a high level of long-chain n-3 polyunsaturated fatty acids (LC n-3 PUFA), mainly eicosapentaenoic acid (EPA) and docosahexaenoic acid (DHA), such as fish oil, are potentially effective adjuncts for cancer treatment with minimal or no side effects [9]. Krill oil (KO), extracted from Antarctic krill (*Euphasia superba*), is also a rich source of LC n-3 PUFA. It is different from fish oil since EPA and DHA in KO are mainly bound to phospholipids instead of triglycerides as in fish oil [10, 11]. This suggests the potentially higher bioavailability of KO-derived LC n-3 PUFA compared to fish oil. In addition, KO contains the antioxidant astaxanthin, vitamins, and minerals [11]. Several animal studies and human trials have reported various health benefits of KO, including its anti-inflammatory properties [12] and its therapeutic effects on glucose metabolism [13], brain disorders [14], cardiovascular diseases [15], as well as CRC [16].

Zhu et al. [17] and Su et al. [18] reported the anti-proliferative properties of KO on CRC and osteosarcoma cells. Our previous in vitro studies demonstrated that free fatty acid extract (FFAE) of KO inhibits the proliferation and induces the death of CRC cells through alteration of mitochondrial membrane potential, leading to DNA damage and apoptosis [19, 20]. Furthermore, Zhen et al. [21] found that EPA and DHA of KO possess a special E-configuration associated with a high anti-proliferative activity observed in several types of cancer cells.

Programmed death-ligands (PD-Ls), PD-L1 and PD-L2, expressed on the surface of tumour cells play a major role in suppressing the immune response and, therefore, providing an immune escape mechanism for cancer progression. The binding of PD-Ls to a programmed cell death protein 1 (PD-1), an immune checkpoint protein expressed on activated T cells, B cells, and myeloid-derived dendritic cells, initiates immunosuppressive signalling pathways [22, 23]. The interaction between the PD-1 with PD-Ls inhibits T cell function, and therefore, provides a favourable environment for the tumour cells

to evade immune response [22, 23]. Our previous study found that the FFAE of KO suppresses PD-L1 expression in CRC cells [24]. Heat shock proteins (HSPs) are highly preserved molecular chaperones found in all living organisms. They play different roles in the various cellular processes [25]. HSP-70 is a powerful anti-apoptotic protein that suppresses mitochondrial damage and DNA fragmentation by reducing caspase activation [26, 27]. Overexpression of HSP-70 increases tumorigenicity and promotes cancer cell growth [28, 29]. Upregulation of HSP-70 correlates with the advanced clinical stages, metastatic spread, and poor survival of CRC patients [30], indicating that HSP-70 may be a potential therapeutic target for CRC treatment. Cai et al. [31] have demonstrated that treatment with DHA in combination with celecoxib inhibits prostate cancer cell growth by mediating protein-protein interactions between HSP70 and p53. However, Chung et al. [32] showed no change in HSP-70 level in prostate cancer cells following n-3 PUFA treatment.

There is little information available on the anti-cancer properties of KO in vivo and the associated molecular mechanisms. A previous study showed that KO treatment inhibits tumour growth in mice bearing human colon cancer xenografts, but the mechanisms of its anti-cancer effects have not been determined [16]. The aims of this study are to (i) investigate the effect of KO supplementation on CRC tumour growth and metastasis in comparison with oxaliplatin treatment; (ii) determine whether the in vivo anti-cancer effect of KO is associated with the mitochondrial death pathway, and (iii) investigate the in vivo effect of KO on the expression of PD-L1, PD-L2, PD-1, and HSP-70. To the best of our knowledge, this is the first animal study comparing the efficacy of KO supplementation with oxaliplatin on CRC growth and metastasis, and investigating the potential molecular targets of KO.

Material and methods

Cell culture

The CT-26 mouse colon adenocarcinoma cell line was obtained from the American Type Culture Collection (ATCC), Manassas, VA, USA (Catalogue No. CRL-2638). Cells were cultured in RPMI1640 medium (Sigma Aldrich, Castle Hill, NSW, Australia) supplemented with fetal calf serum (FCS, 10%) (Hyclone Quantum Scientific, Clayton South, VIC, Australia) and 4-2-hydroxyethyl-1-piperazineethanesulfonic acid, glutamine (10 mM), penicillin (100 U/mL)/streptomycin (100/mL) and sodium pyruvate (10 mM) (Sigma Aldrich, Castle Hill, NSW, Australia). Cells were maintained in a humidified atmosphere in 5% CO₂, 95% air at 37 °C. More than 90%

of viable cells obtained after trypsinization of the monolayer culture were used to make the injection. The cell viability was ensured by the trypan blue exclusion assay.

Experimental model

The animal study was approved by the Victoria University Animal Ethics Committee (AEC No.17/008). The mice were maintained in accordance with the guidelines of the Australian National Health and Medical Research Council Code of Conduct on the care and use of laboratory animals for scientific purposes. Balb/c mice ($n=36$, 6–7 weeks old, weighted 18–25 g) were obtained from the Animal Resource Center (Perth, Australia). Upon arrival, animals were randomized into six groups of six mice in each [sham (control) group and five treatment groups] and housed in OptiMouse cages under pathogen-free conditions with a 12 h light/dark cycle in a well-ventilated room at 22 °C with free access to food and water.

Treatments

At the end of the 5-day acclimatization period, treatments were introduced 3 weeks before CRC induction and continued for 3 weeks post-surgery (Fig. 1). Group 1 (sham) was fed with a standard rodent diet (manufactured by Specialty Feeds, Western Australia) prior to and after cancer induction. Group 2 (positive control) received a rodent diet supplemented with 150 g/kg of corn oil (Gold Fish Brand, Australia) prior to and after cancer induction. Group 3 (positive control) was given a rodent diet supplemented with 150 g/kg of corn oil prior to cancer induction and the same concentration of corn oil combined with intraperitoneal injections of $\frac{1}{2}$ dose of oxaliplatin (1.5 mg/kg, Tocris Bioscience, UK) 3 times/week starting at day 5 post-surgery for 2 weeks. Group

4 received a rodent diet supplemented with 150 g/kg of KO (Swisse Wellness Pty Ltd., Victoria, Australia) prior to and after cancer induction. Group 5 was supplemented with 150 g/kg of KO prior to cancer induction and the same concentration of KO combined with intraperitoneal injections of $\frac{1}{2}$ dose of oxaliplatin 3 times/week starting at day 5 post-surgery for 2 weeks. Group 6 received a standard rodent diet and intraperitoneal injections of a full dose of oxaliplatin (3 mg/kg) 3 times/week starting at day 5 post-surgery for 2 weeks. Groups 1, 2 and 4 received intraperitoneal injections of 200 μ L of sterile saline 3 times/week starting at day 5 post-surgery for 2 weeks. KO contains 13% EPA, 7.5% DHA and 0.03% Astaxanthin. The percentage of KO supplemented in the feed (150 g/kg) was determined as the most effective dose based on the pilot study results (unpublished data). The amount of oil provided to animals was calculated based on their feed consumption rate (g/day) and adjusted regularly. Oil supplement was mixed with the standard rodent diet by loading into a pre-calibrated hole in the pellet. KO and corn oil containing diets were prepared fresh and replaced daily to minimize the oxidation of polyunsaturated fatty acids. The consumption of feed was measured daily, and body weight was recorded twice a week.

Orthotopic CRC induction

At the end of 3-week treatment, CT-26 cells (1×10^6 cells in 25 μ L Matrigel, Sigma, Australia) were injected into the caecum of mice to induce cancer as described before [33]. After 21 days of tumour inoculation, or when the tumour size was over 1 cm³, the animals were culled by overdosing with pentobarbitone (100 mg/kg). Kaplan Meier survival analysis was used to assess the survival rate of animals in each group. Immediately after mice

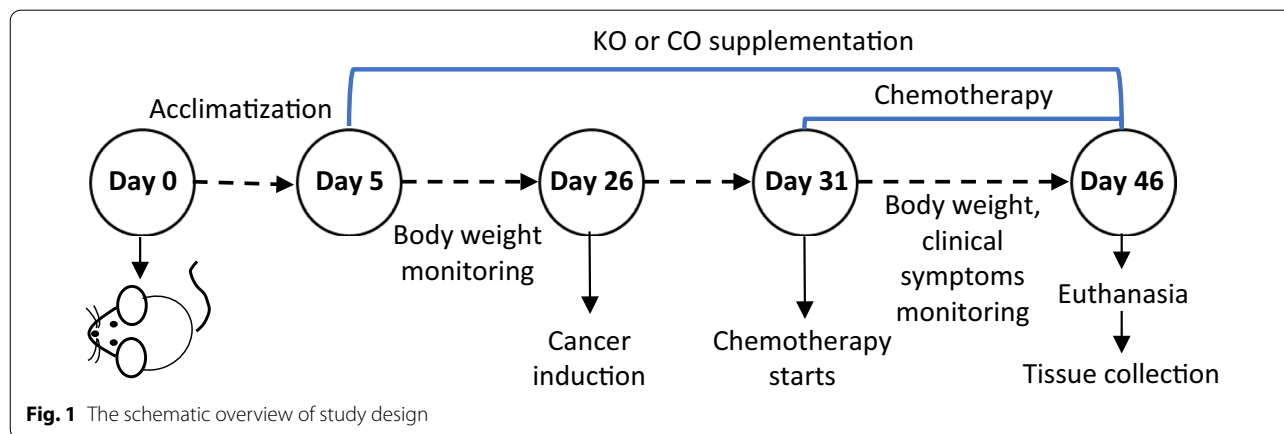


Fig. 1 The schematic overview of study design

were sacrificed, their body was dissected and metastases were identified via visual observation. The number of tumours were counted and recorded in all organs including skin and muscles. The tumour samples were immediately removed. Approximately 1/3 of tumour tissues were snap-frozen in liquid nitrogen and stored at -80°C until further analysis by Western blotting, remaining 2/3 of tumour tissues were incubated overnight in Zamboni's fixative [2% formaldehyde, 0.2% picric acid, and 0.1 M sodium phosphate buffer (pH 7)] at 4°C for immunohistochemical or histological analysis.

Histology

Zamboni's fixed tissues were washed 3×10 min with dimethyl sulfoxide (DMSO) (Sigma, Australia) and 3×10 min with phosphate-buffered saline (PBS). Tissues were embedded in paraffin, sectioned at $5 \mu\text{M}$ and used for a standard Haematoxylin and Eosin (H&E) staining. Initially, sections were immersed in xylene (3×4 min), followed by 3 min in 100% ethanol, 2 min in 90% ethanol, 2 min in 70% ethanol, and washed with tap water. Then they were immersed for 4 min in Harris Haematoxyline (Richard Allan Scientific, USA), rinsed with tap water, followed by 1 min in Scott's tap water, immersed in 1% Eosin (Amber Scientific, Australia) for 3 min, rinsed in tap water, 100% ethanol (2×1 min), xylene (2×3 min), and mounted on the distyrene plasticizer xylene (DPX) with a coverslip. The histological slides were observed under a fluorescent microscope. Each slide was analysed by randomly capturing 10 sections per preparation at $20 \times$ magnification using a DP72 camera and processed using cellSens standard 1.4.1 software (Olympus, Australia). The tumour cells counterstained with Haematoxylin stain were quantified within an area of 2 mm^2 using the Image J software (National Institute of Health, USA). Five different histological samples from each mouse were examined and the number of tumour cells was averaged to obtain the final results. All images were analysed blindly.

Immunohistochemistry

After 24 h of fixation in Zamboni's solution, tumour tissues were washed with 100% DMSO (Sigma-Aldrich, Australia) 3×10 min to remove the fixative, and this was followed by 3×10 min washing with PBS. Then samples were embedded in an Optimum Cutting Temperature compound (OCT Sakura, Tissue Tek, USA) and sectioned at a thickness of $10 \mu\text{M}$ using a cryostat (Leica CM 1950, Biosystems, Germany). The tissues were mounted onto microscopic slides (Superfrost^R Plus, Thermo Fisher Scientific, Australia) and incubated with 10% donkey serum for 1 h at room temperature to block the endogenous peroxidase activities. Following

the washing with PBS, tumour sections were incubated overnight at room temperature in a humidified atmosphere with primary antibodies for cytochrome *c* (1:1000, rabbit mAb, Abcam 133,504 [EPR 1327], USA), cleaved caspase-9 (1:500, rabbit mAb, Asp 330 [E5Z7N], Cell Signaling Technologies, USA), cleaved caspase-3 (1:500, rabbit mAb, Asp175 [5A1E], Cell Signaling Technologies, USA), DNA/RNA damage (1:500, anti-8-OHdG mouse mAb [15A3], Abcam, USA), PD-L1 (1:500, rabbit mAb, [ab213480], Abcam, USA), PD-L2 (1:500, rabbit, ab187662, Abcam, USA), PD-1 (1:500, rat [clone RPM1-14], Bio-Cell, USA), HSP-70 (1:500, mouse mAb, ab2787, Abcam, USA). On the following day, the slides were washed 4×10 min with PBS-T (PBS + 0.1% Tween-20) and incubated with secondary antibodies (diluted to 1:250) labeled with different fluorophores: Alexa Fluor 594 and 488 conjugated donkey anti-rabbit (Jackson Immuno Research Laboratories, USA), Alexa Fluor 488-conjugated donkey anti-mouse (Jackson Immuno Research Laboratories, USA) and Alexa Fluor 594-conjugated donkey anti-rat (Jackson Immuno Research Laboratories, USA) at room temperature for 2 h. This was followed by 4×10 min washes with PBS-T. Then the slides were incubated with a fluorescent nucleic acid stain, 4',6'-diamidino-2-phenylindole dihydrochloride (DAPI, 14 nM, Life Technologies, Australia) for 2 min. Finally, all slides were washed with PBS for 10 min and cover-slipped using a fluorescent mounting medium (DAKO, Australia). Images were taken with the Eclipse Ti confocal laser scanning system (Nikon, Tokyo, Japan). The excitation wavelengths for FITC and Alexa Fluor 594 were adjusted to 488 nm and 559 nm, respectively. Each fluorophore was measured using 8 images taken at $40 \times$ magnification with a total area of 1 mm^2 . All images were then calibrated to standardize for a minimum basal fluorescence and converted to binary. Fluorescence intensity was measured using Image J software (National Institute of Health, USA). The results were verified through at least three individual repeated experiments. All slides were coded, and analysis was performed blindly.

Western blot

Frozen pooled tumour samples ($n=6$ mice/group) were homogenized using a Polytron homogenizer (Kinematica AG, Switzerland) for 15 s in ice-cold radioimmunoprecipitation assay (RIPA) buffer (pH 7.4, 150 mM NaCl, 0.1% SDS, 0.5% sodium deoxycholate, 1% NP-40 in PBS, Sigma, Australia) containing a protease and phosphatase inhibitors cocktail (Roche Applied Science, USA). The lysis was centrifuged at 12,000 rpm for 20 min at 4°C and supernatants were used for western blot analysis. Protein concentration was determined

by the Pierce bicinchoninic acid (BCA) assay (Thermo Fisher Scientific, Australia). Protein samples were loaded as 12 µg/lane onto Mini-PROTEAN® TGX™ (4–20%) stain-free precast gel (Bio-Rad, USA) and separated by 10% sodium dodecyl sulfate polyacrylamide gel electrophoresis (SDS-PAGE). The separated fragments were transferred to 0.22 µm polyvinylidene fluoride membranes, which were blocked with 5% skim milk in PBST (0.1% Tween-20) by incubating at room temperature at 40 rpm speed shaker for 90 min. Then the membrane was incubated with primary antibodies against cytochrome *c* (1:1000, rabbit, Abcam 133,504 (EPR 1327), USA), cleaved caspase-9 (1:1000, rabbit mAb, Asp 330 (E5Z7N), Cell Signaling Technologies, USA), cleaved caspase-3 (1:1000, rabbit mAb, Asp175 (5A1E), Cell Signaling Technologies, USA), DNA/RNA damage (1:500, mouse anti-8-OHdG mAb, (15A3), Abcam, USA), PD-L1 (1:1000, rabbit mAb, Cell Signaling Technologies, USA), PD-L2 (1:1000, rabbit, Cell Signaling Technologies, USA), and GAPDH as a control (1:2000 dilution, rabbit, Santa Cruz Biotechnology, USA) overnight at 4 °C. The membrane was washed four times in PBS-T (0.1% Tween-20) and incubated with horseradish peroxidase (HRP)-conjugated secondary antibodies, donkey anti-rabbit IgG (1:10,000, 31,458, Thermo Fisher Scientific, Australia), and horse anti-mouse IgG (1:10,000, Cell Signaling Technology, USA) for 2 h at room temperature. Again, the membrane was washed three times in PBS-T. To detect the protein levels, the membrane was incubated with clarity enhanced chemiluminescence reagents (Clarity™ Western ECL Substrate, Bio-Rad, USA) for 5 min. Chemiluminescence signals were captured using the FUSION FX System (USA). The expression level of each protein was quantified using Fusion Capt advanced FX7 software.

Statistical analysis

All data were analysed using SPSS 22 software (IBM, USA). Mixed model ANOVA was used to determine the significance between treatments. The significance of repeated measures at different time points was analysed using one-way ANOVA. Post-hoc analysis was conducted using the Tukey HSD test for multiple comparisons. $P < 0.05$ was considered significant. The Kaplan Meier survival analysis was performed to assess the survival rate of animals in each group using the formula: Survival Rate = (number of subjects living at the start – number of subjects died) / number of subjects living at the start. One-way ANOVA was performed to compare the survival rate of animals in different experimental groups. The results were expressed as mean ± SD in tables and mean ± SEM in figures.

Results

The effects of KO supplementation on mouse survival rate and tumour growth

The effects of KO supplementation, alone or combined with a ½ dose of oxaliplatin, in Balb/c mice were compared to corn oil treatment groups (corn oil alone or combined with a ½ dose of oxaliplatin), sham (control) group, and a full dose of the oxaliplatin treatment group. No significant difference in the body weight was observed between any groups, although the oxaliplatin-treated group had the lowest body weight gain (Fig. 2A). There were no significant difference in food intake among treatment groups before or after CRC induction. The average food intake before CRC induction ranged between 2.4 and 2.5 g/day among the treatment groups, while after CRC induction it was 2.4 g/day for sham group, 2.2 g/day for both corn oil and corn oil + 1/2 oxaliplatin groups, 2.5 g/day for krill oil group, 2.6 g/day for krill oil + ½ oxaliplatin group, and 2.2 g/day for oxaliplatin group. The survival rate of animals supplemented with KO alone, KO combined with a ½ dose of oxaliplatin, and a full dose of oxaliplatin was significantly higher compared to the sham group (Fig. 2B). It was also noticed that the survival rate of animals from the two KO treatment groups (KO alone or in combination with ½ dose of oxaliplatin) was similar to the survival rate of animals treated with the full dose of oxaliplatin. Moreover, animals from KO supplemented groups did not show any noticeable side effects compared to the animals received the full dose of oxaliplatin which had a poor appetite, were lethargic, and less active.

The results of the histological examination of tumours collected from all groups (Fig. 2C) are presented in Fig. 2D. The number of tumour cells was significantly reduced following treatments with KO alone, KO combined with a ½ dose of oxaliplatin, as well as oxaliplatin alone, with a 53.5%, 58.8% and 53.9% decrease being observed respectively compared to the sham group. In contrast, no change in the number of tumour cells was observed in animals treated with corn oil, either alone or in combination with ½ dose of oxaliplatin compared to the sham group (Fig. 2D).

There were no significant changes in the total mean weight and volume of tumour between the two corn oil groups (corn oil alone and corn oil combined with a ½ dose of oxaliplatin) and the sham group at the end of the treatment period ($P > 0.05$) (Fig. 2E, F). In contrast, animals receiving KO treatment showed significantly reduced tumour weight (0.83 ± 0.2 g vs. 2.63 ± 0.2 g in the sham group and 2.73 ± 0.3 g in corn oil group) and

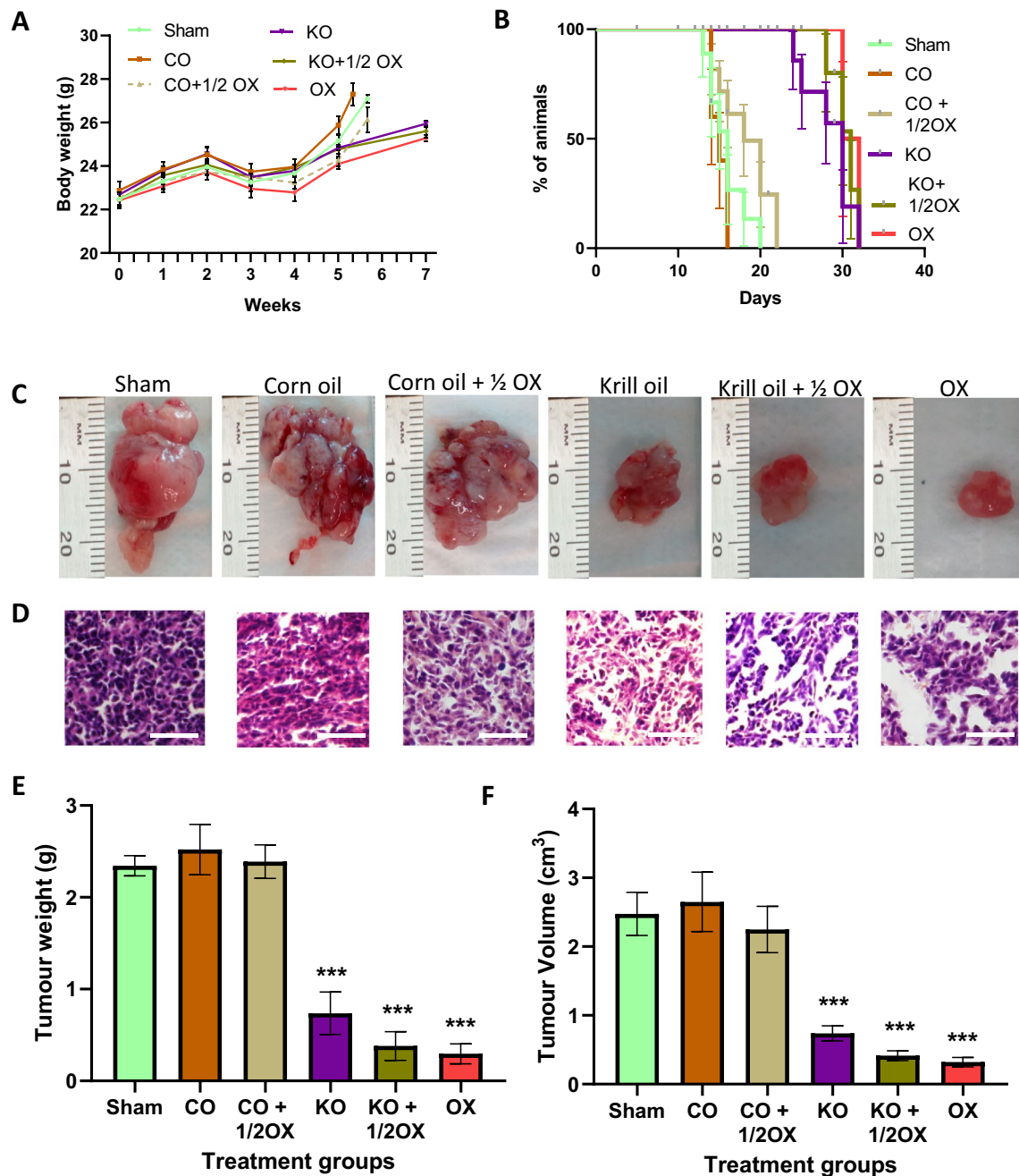


Fig. 2 Effects of treatments on the body weight, survival rate, and tumour growth in Balb/c mice with orthotopic CRC. **A** The effects of treatments on the animal body weight. **B** Kaplan–Meier survival plot representing the percentage of survival of mice after treatment. **C** Representative images of orthotopic tumours excised from different treatment groups. **D** Representative histology images of tumour tissues (H&E stained, Magnification = 20X). **E** The mean tumour weight and **F** volume following various treatments. N = 6 mice per group. The results are expressed as mean ± SEM; ****P* < 0.001 compared to the sham group

volume ($0.74 \pm 0.1 \text{ cm}^3$ vs. $2.5 \pm 3.1 \text{ cm}^3$ in the sham group and $2.7 \pm 0.4 \text{ cm}^3$ in the corn oil group) (*P* < 0.001 for both). These represent a 69.3% reduction in tumour weight and a 70.1% reduction in tumour volume

compared to the sham group. Similarly, compared with the corn oil group, the tumour weight was reduced by 69.6%, and tumour volume by 72.1%. Further reduction was observed in animals received KO and KO combined

with a ½ dose of oxaliplatin, with 0.42 ± 0.1 g being recorded for tumour weight and 0.4 ± 0.1 cm³ for tumour volume, indicating a reduction of 84.2% and 83.3%, respectively, compared to the sham group ($P < 0.001$ for both). For animals treated with a full dose of oxaliplatin, the average tumour weight and volume were 0.37 ± 0.1 g and 0.3 ± 0.1 cm³ respectively ($P < 0.001$ for both), indicating a reduction of 85.9% in tumour weight and 87.1% in tumour volume compared to the sham group (Fig. 2E, F). The differences between two KO -treated groups and a full dose of the oxaliplatin-treated group were not statistically different ($P > 0.05$), indicating that treatment with KO alone or KO combined with a ½ dose of oxaliplatin achieved similar outcomes as a full dose of oxaliplatin treatment.

The effect of KO supplementation on tumour metastasis

Mice in the sham group showed an aggressive tumour growth and metastasis in the abdomen and various organs, including the small intestine, colon, liver, spleen, kidneys, and diaphragm. Mice from the groups received corn oil and corn oil with ½ dose of oxaliplatin also exhibited extensive tumour growth and metastasis, similar to the sham group. In contrast, two out of six mice treated with KO showed reduced metastasis compared to the sham animals. The most noticeable effects on metastasis were observed in animals treated with KO combined with a ½ dose of oxaliplatin, with only one out of six animals showing tumour metastasis and the remaining five animals having no detectable metastasis. Furthermore, the number of metastasized locations and the size of tumours were reduced significantly, similar to the oxaliplatin-treated group compared to the sham group.

Expression of cytochrome c, caspase-9, caspase-3, and DNA damage in tumours following KO treatment

Figure 3 shows the effects of treatments on the expression of cytochrome c and cleaved caspase-9 in tumour tissues. Animals treated with KO alone, KO combined with a ½ dose of oxaliplatin, and a full dose of oxaliplatin showed a significantly higher cytochrome c expression [61.3% ($P < 0.001$), 78.15% ($P < 0.001$), and 19.25%

($P < 0.05$), respectively] compared to the sham group (Fig. 3A, C). These three treatments also resulted in a significantly higher expression of cleaved caspase-9 in tumours with an increase of 85.2% ($P < 0.001$), 68.4% ($P < 0.001$), and 21.3% ($P < 0.05$), respectively (Fig. 3B, D). The results of the expression of cytochrome c and cleaved caspase-9 observed through western blotting (Fig. 3E) were consistent with the findings of the immunohistochemistry assay.

Furthermore, KO treatment significantly increased the expression of cleaved caspase-3 by 92.93% compared to the sham group ($P < 0.001$) (Fig. 4A, C). Treatment with KO combined with a ½ dose of oxaliplatin increased the expression of cleaved caspase-3 by 77.95% ($P < 0.01$), and the full dose of oxaliplatin by 41.73% ($P < 0.05$). DNA damage was also significant compared to the sham group, with an increase of the DNA damage resulting from the treatment with KO alone, KO combined with a ½ dose of oxaliplatin and a full dose of oxaliplatin by 48.3%, 62.4%, and 31.6%, respectively ($P < 0.001$ for all) (Fig. 4B, D). Results of immunohistochemistry assay for the expression of cleaved caspase-3 and DNA damage were further verified by western blotting (Fig. 4E), and consistent results were observed.

Expression of PD-L1, PD-L2, PD-1 and HSP-70 in tumours following the treatment with KO

The animals treated with KO, KO combined with ½ dose of oxaliplatin, and a full dose of oxaliplatin showed a significant reduction of PD-L1 expression in tumours by 57.7% ($P < 0.001$), 46.7% ($P < 0.01$), and 35.3% ($P < 0.05$), respectively, compared to the sham group (Fig. 5A, C). There were no significant differences in the expression of PD-L1 between animals received treatments with KO, KO combined with ½ dose of oxaliplatin, and a full dose of oxaliplatin ($P > 0.05$). Similar results were observed in the expression of PD-L2 following treatments with KO alone, KO combined with ½ dose of oxaliplatin, and a full dose of oxaliplatin with a reduction by 37.6% ($P < 0.01$), 43.5% ($P < 0.01$), and 58.6% ($P < 0.001$), respectively, compared

(See figure on next page.)

Fig. 3 Expression of cytochrome c and cleaved caspase-9 following treatments. The expression of cytochrome c (A) and cleaved caspase-9 (B) in tumours following different treatments determined immunohistochemically using monoclonal antibodies. Quantitative analysis of the fluorescence intensity of cytochrome c (C) and cleaved caspase-9 (D) expression in tumour tissues following various treatments determined by immunohistochemistry. Scale bar = 50 μm. Magnification = 40X. N = 6 mice per group. The level of fluorescence was measured using 8 randomly taken images that provide a total area of 1 mm². The results are expressed as mean ± SEM; * $P < 0.05$, *** $P < 0.001$ compared to the sham group; ^^^ $P < 0.001$ compared to the oxaliplatin-treated group. E The expression of cytochrome c and cleaved caspase-9 measured by western blotting in tumours from different treatment groups

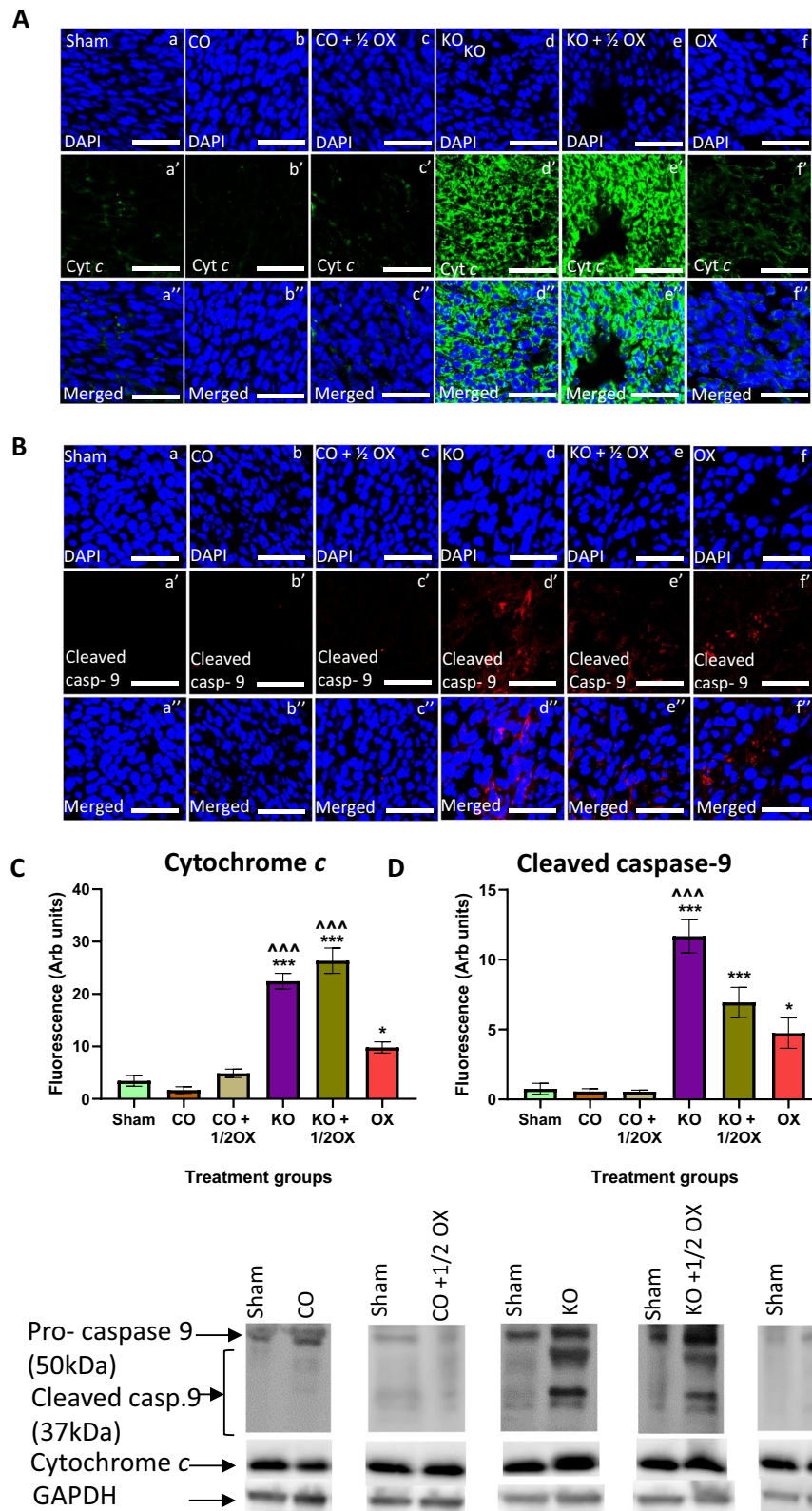


Fig. 3 (See legend on previous page.)

to the sham animals (Fig. 5B, D). The expression of PD-L2 was not significantly different between the animals that received treatments with KO, KO combined with ½ dose of oxaliplatin, and a full dose of oxaliplatin ($P > 0.05$). These results were further confirmed by the western blotting assay as shown in Fig. 5E.

The animals treated with KO showed a significant reduction of PD-1 expression ($P < 0.05$) in tumours compared to the sham group (Fig. 6A, C). The animals treated with KO, KO combined with ½ dose of oxaliplatin, and a full dose of oxaliplatin showed a significant reduction of HSP-70 level ($P < 0.05$ to $P < 0.01$) in the tumours compared to the sham group (Fig. 6B, D).

Discussion

This is the first animal study investigating the anti-cancer efficacy of KO supplementation on CRC in comparison with the currently used chemotherapeutic agent, oxaliplatin. This study demonstrated that treatments with KO and KO combined with a ½ dose of oxaliplatin increased the survival rate of mice with CRC in a similar manner as the full dose of oxaliplatin. The results showed that treatment with KO alone significantly reduced tumour weight by 69% and volume by 70%, while KO combined with a ½ dose of oxaliplatin reduced tumour weight by 84% and volume by 83%. More significantly, we found that KO combined with a ½ dose of oxaliplatin reduced tumour size and metastasis at a similar rate with no noticeable side effects compared to the full dose of oxaliplatin where animals showed a reduced appetite, lethargy and weakness. Oxaliplatin-induced side effects observed in this study are consistent with previous reports from our and other groups [8, 9, 34, 35]. In addition, this study showed that treatments with KO, KO combined with a ½ dose of oxaliplatin, and a full dose of oxaliplatin resulted in a high level of expression of cytochrome *c* released from mitochondria in the tumours. These treatments also increased the expression of cleaved caspase-9 and cleaved caspase-3, and DNA damage in tumours. Furthermore, the expression of PD-L1, PD-L2 and HSP-70

was reduced significantly in the tumour tissue of mice received those three treatments. The lower expression of PD-1 was also observed in the animals treated with KO.

Gastrointestinal and neurological complications are well documented as side effects resulting from oxaliplatin treatment in CRC [36]. To overcome these issues, one of the most common practices is dose or frequency reduction with chemotherapy treatment. This could provide a better adaptation to the chemotherapeutic drug with fewer side effects and could encourage patients to continue treatment for a longer period until the desired results are obtained [34]. The fact that animals received the combined treatment of KO with a ½ dose of oxaliplatin increased survival rate and reduced the tumour growth comparably with the full dose of oxaliplatin but without side effects, as demonstrated in this study, suggests a possible interaction of KO and the chemotherapeutic drug. It also implicates the potential role of KO as an adjunctive agent to reduce the side effects associated with oxaliplatin treatment.

KO is a rich source of LC n-3 PUFA, EPA and DHA, as well as antioxidant astaxanthin [11]. Previous studies have investigated the effects of LC n-3 PUFA or fish oil combined with chemotherapeutic agents in the treatment of cancer [35], and identified that combined treatments of LC n-3 PUFA with chemotherapy decreased the required dose of chemotherapeutic agents, hence the side effects associated with higher doses of chemotherapy. The study by Vasudevan et al. [37] reported that EPA administered together with a combination of 5-fluorouracil (5-FU) and oxaliplatin (FuOX) greatly reduced tumour growth in mice with HCT-116 and HT-29 cell xenografts. The authors observed that the reduction in the size of tumour was primarily due to the decrease of tumour cell proliferation attributed to increased sensitivity of tumour cells to the EPA/FuOX combined therapy. Rani et al. [38] investigated the effects of treatment with fish oil combined with 5-FU on CRC and reported that it significantly reduced

(See figure on next page.)

Fig. 4 Expression of cleaved caspase-3 and DNA damage following treatments. The expression of cleaved caspase-3 (A) and DNA damage (B) in tumours following different treatments determined immunohistochemically using monoclonal antibodies. Quantitative analysis of the fluorescence intensity of cleaved caspase-3 (C) and DNA damage (D) expression in tumour tissues following various treatments determined by immunohistochemistry. Scale bar = 50 μ m. Magnification = 40X. N = 6 mice per group. The level of fluorescence was measured using 8 randomly taken images that provide a total area of 1 mm². The results are expressed as mean \pm SEM; * $P < 0.05$, ** $P < 0.01$, *** $P < 0.001$ compared to the sham group; **** $P < 0.001$ compared to the oxaliplatin-treated group. E The expression of cleaved caspase-3 and DNA damage measured by western blotting in tumours following various treatments

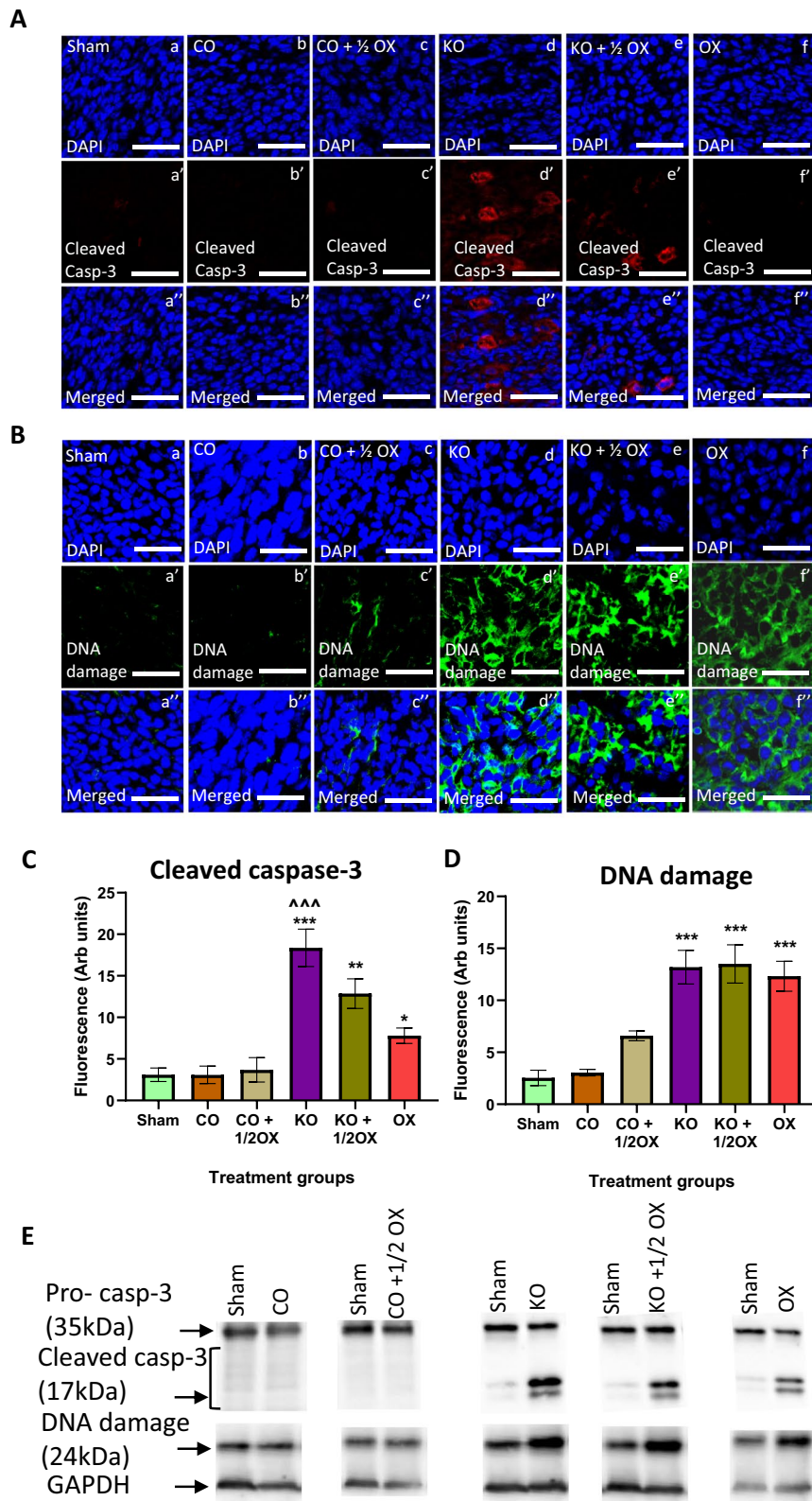


Fig. 4 (See legend on previous page.)

tumour burden and the 5-FU-associated side effects in a model of DMH/DSS-induced colon cancer in Balb/c mice. The authors also observed that fish oil supplementation increased the effectiveness of 5-FU and activated both intrinsic and extrinsic apoptotic pathways in these mice. Based on this evidence, it is likely that LC n-3 PUFA play an important role in the beneficial effects of KO combined with a ½ dose of oxaliplatin observed in the present study.

Astaxanthin is one of the most common carotenoids and has displayed more powerful anti-oxidative properties than other carotenoids. It exerts several important functions in the human body including prevention of oxidation of EPA and DHA, modulation of exacerbated inflammation responses, and control of carcinogenic processes [39, 40]. Previous studies have discovered the beneficial effects of astaxanthin as a therapeutic agent for various diseases without toxicity or side effects. It also showed preclinical anti-tumour effectiveness both in vivo and in vitro [41] in different cancer models such as oral cancer [42], colon cancer [43], bladder cancer [44] and leukemia [45]. The association of astaxanthin with the beneficial effects of KO combined with a ½ dose of oxaliplatin is not clear in the present study. It is possible that both LC n-3 PUFA and astaxanthin in KO play a role. Further animal studies including co-supplementations of isolated bioactive components including EPA, DHA, and astaxanthin combined with oxaliplatin are warranted to understand their specific contribution to the overall anti-cancer properties of KO in vivo.

Cytochrome *c* (Cyt *c*) is a peripheral protein located in the inner membrane of the mitochondria, and it functions as an electron transporter in-between complex iii and complex iv in the respiratory chain [46]. It is produced in the cytosol as an apoprotein and then translocated to the mitochondria. The majority of Cyt *c* is loosely attached to the intermembrane in mitochondria, and the remaining 15% are tightly bound to the inner membrane through electrostatic and hydrophobic interactions [47]. If cells receive apoptotic stimuli in the presence of ATP, Cyt *c* is released from the mitochondria by opening the pores of the outer membrane. Cyt *c* then binds to apoptosis protease activating factor 1 (Apaf-1)

and generates an apoptosome complex [48]. The activated apoptosome can facilitate autocatalytic activation of caspase-9 essential for the initiation of intrinsic apoptosis through stimulation of caspase-3 [49]. The present study found that mice received treatments with KO, KO combined with a ½ dose of oxaliplatin, and the full dose of oxaliplatin had a significantly higher expression of Cyt *c* in tumour tissues. These treatments also increased significantly the level of cleaved caspase-9 and cleaved caspase-3 in tumour tissues. The animals treated with KO alone showed the highest level of cleaved caspase-9 and cleaved caspase-3, followed by those treated with KO combined with a ½ oxaliplatin. These results are consistent with our in vitro observations on CRC cell lines following the treatment with FFAE of KO [19, 20]. The present data provide in vivo evidence that inhibition of CRC tumour growth by KO may occur through the activation of intrinsic mitochondrial death pathway involving the increased release of Cyt *c* and activation of caspase-9 and caspase-3 leading to tumour cell death. These mechanistic impacts of KO are more likely related to its LC n-3 PUFA as demonstrated in our previous in vitro studies [20], although the role of astaxanthin is not clear.

Our results presented in Fig. 4 demonstrate a significantly high level of DNA damage in groups treated with KO alone, KO + ½ OX, and OX alone confirmed by measurement of 8-hydroxy-2'- Deoxyguanosine (8-OHdG). The interaction of reactive oxygen species with the nucleobases of the DNA strand, such as guanine, leads to the formation of 8-OHdG. Based on this evidence, 8-OHdG has been widely used as a biomarker of oxidative stress-induced DNA damage, and measurement of 8-OHdG level is commonly used to evaluate a load of oxidative stress [50]. Our results demonstrate that the level of DNA damage is similar between three treatment groups, KO, KO + ½ OX, and OX, although other markers of oxidative stress-induced apoptosis, Cyt *c* and cleaved caspase 9, are lower in the oxaliplatin-treated group compared to the KO-treated group. These data suggest that the observed DNA damage in the oxaliplatin-treated group involves other mechanisms apart from the intrinsic mitochondrial apoptotic pathway studied in the present study.

(See figure on next page.)

Fig. 5 Expression of PD-L1 and PD-L2 following treatments. The expression of PD-L1 (A) and PD-L2 (B) in tumours following the treatments determined immunohistochemically using monoclonal antibodies. Quantitative analysis of the fluorescence intensity of PD-L1 (C) and PD-L2 (D) expression in tumour tissues following various treatments determined by immunohistochemistry. Scale bar = 50 μM. Magnification = 40X. N = 6 mice per group. The level of fluorescence was measured using 8 randomly taken images that provide a total area of 1 mm². The results are expressed as mean ± SEM; **P* < 0.05, ***P* < 0.01, ****P* < 0.001 compared to the sham group. E The expression of PD-L1 and PD-L2 measured by western blotting in tumours following various treatments

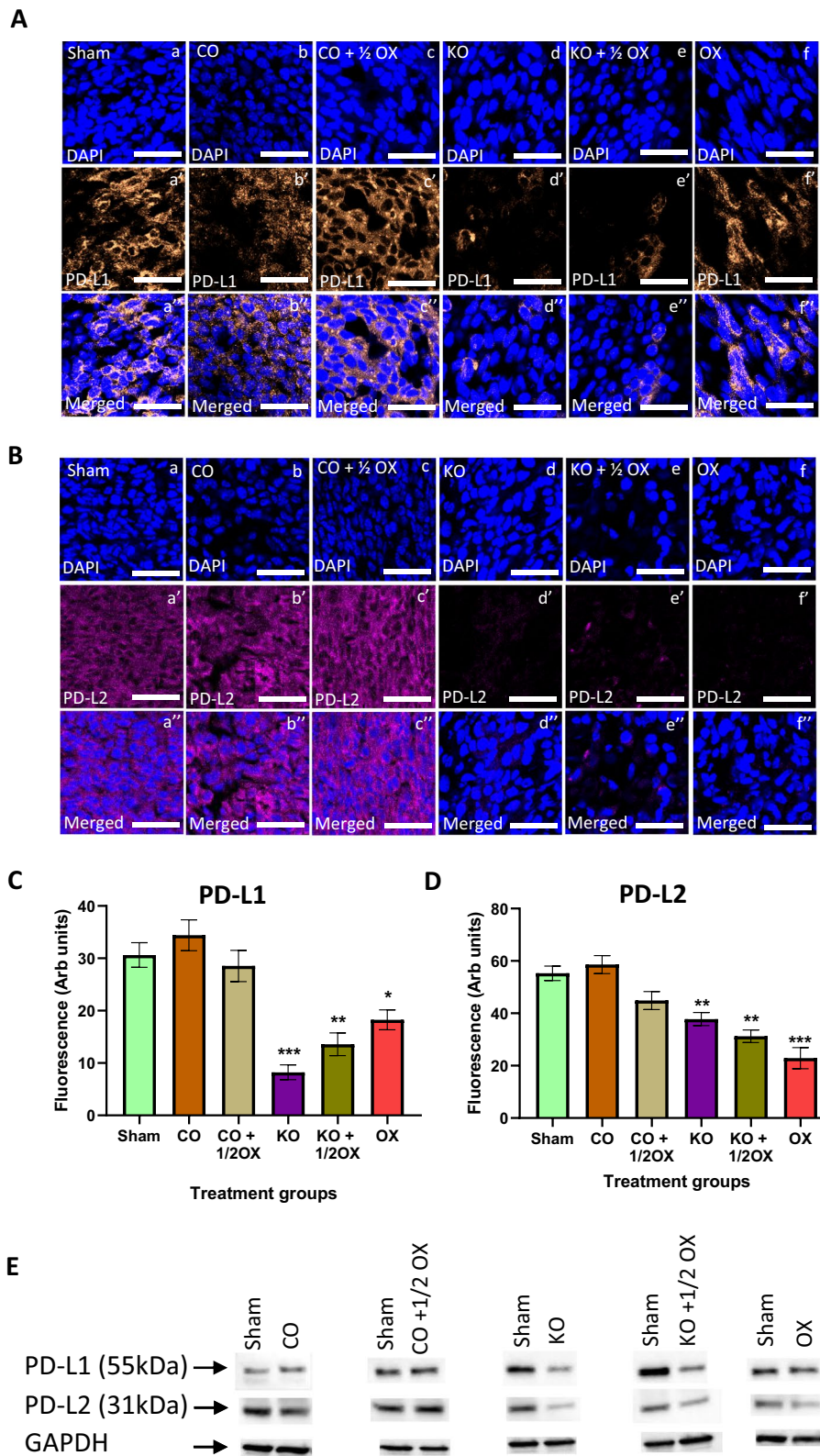


Fig. 5 (See legend on previous page.)

Oxaliplatin exerts its cytotoxic effects mainly through DNA damage leading to apoptosis of cancer cells. DNA damage induced by oxaliplatin can be caused by the formation of DNA lesions due to platinum–DNA adducts, arrest of G1 and G2 phases of the cell cycle, inhibition of mRNA synthesis, and induction of immunogenic cell death [51, 52]. In clinical settings, oxaliplatin is combined with other cytotoxic therapeutic agents with varying degrees of success and severe side effects [9]. Our study demonstrates for the first time that KO supplementation enhances cytotoxic effects of oxaliplatin by augmenting apoptosis of cancer cells via the intrinsic mitochondrial apoptotic pathway. Other studies demonstrated that oxaliplatin induces extrinsic mitochondrial apoptotic pathway via caspase 8 activation in HT-29 colorectal cell line [53]. In addition, the low level of caspase-3 in the oxaliplatin-treated group observed in our study suggests that oxaliplatin might have induced non-apoptotic cell death. Oxaliplatin is a potent inhibitor of survivin, a member of the IAP (inhibitor of apoptosis) family, as shown in colorectal cancer cell lines SW480, DLD1, and HT29 [54]. Dysfunction of survivin induces mitotic catastrophe, a form of non-apoptotic cell death caused by aberrant mitosis and eventually causes slow cell death [55]. Further studies are warranted to elucidate whether KO supplementation augments molecular pathways involved in oxaliplatin-induced apoptotic and non-apoptotic cell death.

PD-L1 and PD-L2 are members of the B7 family of molecules and ligands for PD-1 receptors, which are expressed on activated T and B cells [56]. These two ligands are commonly expressed on T and B cells, dendritic cells, and macrophages, as well as a variety of tumour cells, including CRC cells [57]. The interaction of PD-L1 and PD-L2 with the PD-1 receptor on T cells inhibits T cell proliferation, cytokine production, migration cell adhesion, and finally induces apoptosis [22]. Previous studies showed that blocking of the PD-L1/PD-L2 and PD-1 interaction can reestablish the T cell function and can mediate anti-tumour activity by reducing cancer cell proliferation and migration [58]. Our previous in vitro study showed that the FFAE of KO suppresses the expression of PD-L1 in human CRC cells [24]. The present study is the first demonstrating that KO supplementation downregulates the expression of PD-L1 and

PD-L2 in the tumour tissues from mice with orthotopic CRC in the same manner as a full dose of oxaliplatin. Further studies are required to validate the results observed in this research. Furthermore, the reduction of PD-1 expression in the tumour tissues indicates the enhancement of a pre-existing anti-tumour immune activity due to KO treatment. We also found a reduction in the level of HSP-70 in the tumours from mice treated with KO, KO combined with a ½ dose of oxaliplatin, and the full dose of oxaliplatin. No studies on the effects of KO and n-3 PUFA on the expression of HSP-70 in CRC have been performed previously. HSPs are the most abundant cellular proteins involved in protein stability [59]. The studies found that HSPs are highly expressed in various types of cancer, and that leads to cancer cell proliferation, differentiation, invasion and metastasis [25]. HSP-70 is a stress response protein that can inhibit the apoptosis of cancer cells. Furthermore, the overexpression of HSP70 is shown to increase tumorigenicity [25, 60]. Taken together, our results indicate that KO has the potential to suppress CRC development through the inhibition of PD-L1/PD-L2 interaction with PD-1 and HSP-70.

Based on the findings from this study, supplementations with 150 g/kg of KO, and KO combined with ½ dose of oxaliplatin resulted in significant benefits against CRC in the mouse model with no noticeable side effects. Clinical trials are warranted to determine the efficacy and dosage of this natural product in the prevention and attenuation of CRC in humans.

Conclusion

This study showed that KO supplementation significantly reduced colorectal tumour growth in vivo compared to sham treatment. Combined treatment with KO and ½ dose of oxaliplatin exhibited a significant anti-tumour effect and reduced tumour metastasis at a similar rate as the full dose of oxaliplatin without adverse side effects. The tumor-suppressive effect of KO observed in this in vivo study is likely associated with its anti-proliferative, apoptotic, and anti-inflammatory functions via activation of the intrinsic mitochondrial death pathway. These findings provide preclinical evidence for the anti-cancer properties of KO and its potential role as an effective adjunctive therapy for CRC.

(See figure on next page.)

Fig. 6 Expression of PD-1 and HSP-70 following treatments. The expression of PD-1 (A) and HSP-70 (B) in tumours following various treatments determined immunohistochemically using monoclonal antibodies. Quantitative analysis of the fluorescence intensity of PD-1 (C) and HSP-70 (D) expression in tumour tissues following various treatments determined by immunohistochemistry. Scale bar = 50 μm. Magnification = 40X. N = 6 mice per group. The level of fluorescence was measured using 8 randomly taken images per specimen at 40 × magnification that provide a total area of 1 mm². The results are expressed as mean ± SEM; **P* < 0.05, ***P* < 0.01 compared to the sham group

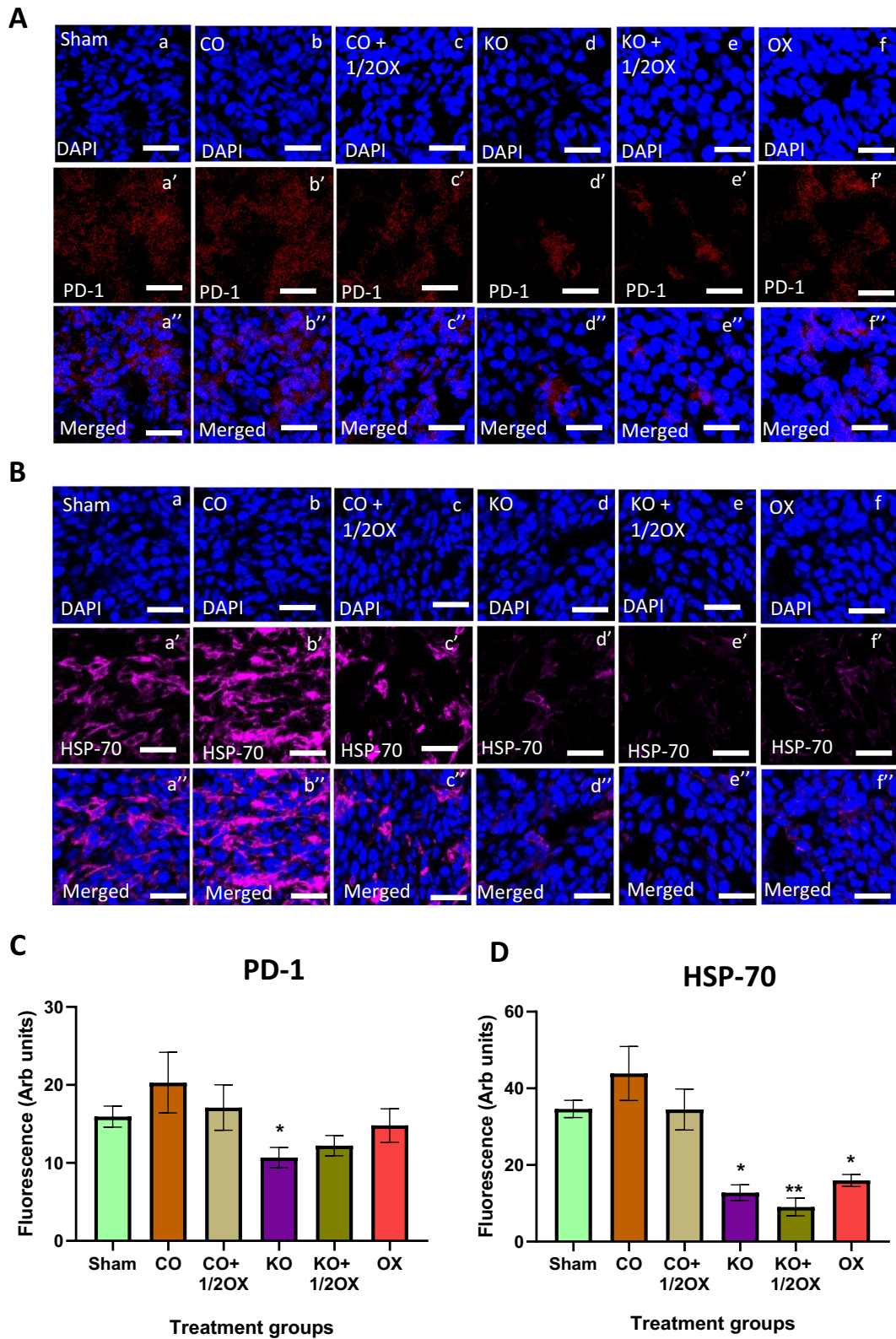


Fig. 6 (See legend on previous page.)

Abbreviations

Apaf-1: Apoptosis protease activating factor 1; ATCC: American tissue culture collection; CO: Corn oil; CRC: Colorectal cancer; Cyt c: Cytochrome c; DAPI: 4,6-Diamidino-2-phenylindole; DHA: Docosahexaenoic acid; DNA: Deoxyribonucleic acid; EPA: Eicosapentaenoic acid; FCS: Foetal calf serum; FFA: Free fatty acids; FFAE of KO: Free fatty acids extractions of KO; GAPDH: Glycereraldehydes-3-phosphate de-hydrogenase; GI: Gastrointestinal; H&E: Haematoxylin and Eosin; HEPES: 4-2-Hydroxyethyl-1-piperazineethanesulfonic; HEPES: 4-2-Hydroxyethyl-1-piperazineethanesulfonic; HSP-70: Heat shock protein-70; KO: Krill oil; LC n-3 PUFA: Long chain n-3 poly unsaturated fatty acid; OCT: Optimal cutting temperature compound; OX/OXAL: Oxaliplatin; PBS: Phosphate-buffered saline; PBS-T: Phosphate-buffered saline + Tween 20; PD-1: Programmed death receptor; PD-L1: Programmed death ligand-1; PD-L2: Programmed death ligand-2; PUFA: Polyunsaturated fatty acids; RIPA: Radioimmunoprecipitation assay buffer; RNA: Ribonucleic acid; SD: Standard deviation; SDS: Sodium dodecyl sulphate; SEM: Standard error of mean.

Acknowledgements

The authors would like to thank Miss Nicole Christie for her assistance in monitoring animals during the study.

Authors' contributions

XS and KN designed the study. AJ collected and analyzed the data and drafted the manuscript. MH assisted with animal experiments, data collection and manuscript preparation, VJ assisted with animal experiments and data collection. XS, KN and RL are responsible for data interpretation and critical revision of the manuscript. All authors read and approved the final manuscript.

Funding

Open Access funding enabled and organized by CAUL and its Member Institutions This study was supported by Victoria University postgraduate research scholarship for AJ.

Availability of data and materials

The datasets used and/or analysed during the current study are available from the corresponding author on reasonable request.

Declarations

Ethics approval and consent to participate

All animal studies were approved by the Victoria University Animal Ethics Committee (AEC No.17/008).

Consent for publication

No applicable.

Competing interests

The authors declare that they have no competing interests.

Author details

¹Institute for Health and Sport, Victoria University, P.O. Box 14428, Melbourne 8001, Australia. ²Department of Surgery, The Royal Melbourne Hospital, The University of Melbourne, Parkville, Australia. ³Department of Medicine-Western Health, The University of Melbourne, Melbourne, Australia. ⁴Regenerative Medicine and Stem Cells Program, Australian Institute for Musculoskeletal Science (AIMSS), Melbourne, Australia.

Received: 15 August 2021 Accepted: 9 February 2022

Published online: 02 March 2022

References

- Araghi M, Soerjomataram I, Jenkins M, Brierley J, Morris E, Bray F, et al. Global trends in colorectal cancer mortality: projections to the year 2035. *Int J Cancer*. 2019;144(12):2992–3000.
- Kwong LN, Dove WF. APC and its modifiers in colon cancer. *Adv Exp Med Biol*. 2009;656:85–106.
- Li J, Yuan Y, Yang F, Wang Y, Zhu X, Wang Z, et al. Expert consensus on multidisciplinary therapy of colorectal cancer with lung metastases (2019 edition). *J Hematol Oncol*. 2019;12(1):16.
- Riihimaki M, Hemminki A, Sundquist J, Hemminki K. Patterns of metastasis in colon and rectal cancer. *Sci Rep*. 2016;6:29765.
- Andre N, Schmiegel W. Chemoradiotherapy for colorectal cancer. *Gut*. 2005;54(8):1194–202.
- Boussios S, Pentheroudakis G, Katsanos K, Pavlidis N. Systemic treatment-induced gastrointestinal toxicity: incidence, clinical presentation and management. *Ann Gastroenterol*. 2012;25(2):106–18.
- McQuade RM, Stojanovska V, Abalo R, Bornstein JC, Nurgali K. Chemotherapy-induced constipation and diarrhea: pathophysiology, current and emerging treatments. *Front Pharmacol*. 2016;7:414.
- Robinson AM, Stojanovska V, Rahman AA, McQuade RM, Senior PV, Nurgali K. Effects of oxaliplatin treatment on the enteric glial cells and neurons in the mouse ileum. *J Histochem Cytochem*. 2016;64(9):530–45.
- Calvani M, Pasha A, Favre C. Nutritional boom in cancer: inside the labyrinth of reactive oxygen species. *Int J Mol Sci*. 2020;21(6):1936.
- Sung HH, Sinclair AJ, Lewandowski PA, Su XQ. Postprandial long-chain n-3 polyunsaturated fatty acid response to krill oil and fish oil consumption in healthy women: a randomised controlled, single-dose, crossover study. *Asia Pac J Clin Nutr*. 2018;27(1):148–57.
- Tou JC, Jaczynski J, Chen YC. Krill for human consumption: nutritional value and potential health benefits. *Nutr Rev*. 2007;65(2):63–77.
- Batetta B, Griinari M, Carta G, Murru E, Ligresti A, Cordeddu L, et al. Endocannabinoids may mediate the ability of (n-3) fatty acids to reduce ectopic fat and inflammatory mediators in obese Zucker rats. *J Nutr*. 2009;139(8):1495–501.
- Sun D, Zhang L, Chen H, Feng R, Cao P, Liu Y. Effects of Antarctic krill oil on lipid and glucose metabolism in C57BL/6J mice fed with high fat diet. *Lipids Health Dis*. 2017;16(1):218.
- van der Wurff ISM, von Schacky C, Bergeland T, Leontjevas R, Zeegers MP, Jolles J, et al. Effect of 1 year krill oil supplementation on cognitive achievement of Dutch adolescents: a double-blind randomized controlled trial. *Nutrients*. 2019;11(6):1230.
- Hals PA, Wang X, Xiao YF. Effects of a purified krill oil phospholipid rich in long-chain omega-3 fatty acids on cardiovascular disease risk factors in non-human primates with naturally occurring diabetes type-2 and dyslipidemia. *Lipids Health Dis*. 2017;16(1):11.
- Morin C, Rodriguez E, Blier PU, Fortin S. Potential application of eicosapentaenoic acid monoacylglyceride in the management of colorectal cancer. *Mar Drugs*. 2017;15(9):283.
- Zhu JJ, Shi JH, Qian WB, Cai ZZ, Li D. Effects of krill oil on serum lipids of hyperlipidemic rats and human SW480 cells. *Lipids Health Dis*. 2008;7:30.
- Su XU, Tanalgo P, Bustos M, Dass CR. The effect of krill oil and n-3 polyunsaturated fatty acids on human osteosarcoma cell proliferation and migration. *Curr Drug Targets*. 2018;19(5):479–86.
- Jayathilake AG, Senior PV, Su XQ. Krill oil extract suppresses cell growth and induces apoptosis of human colorectal cancer cells. *BMC Complement Altern Med*. 2016;16(1):328.
- Jayathilake AG, Kadife E, Luwor RB, Nurgali K, Su XQ. Krill oil extract suppresses the proliferation of colorectal cancer cells through activation of caspase 3/9. *Nutr Metab (Lond)*. 2019;16:53.
- Zheng W, Wang X, Cao W, Yang B, Mu Y, Dong Y, et al. E-configuration structures of EPA and DHA derived from *Euphausia superba* and their significant inhibitive effects on growth of human cancer cell lines in vitro. *Prostaglandins Leukot Essent Fatty Acids*. 2017;117:47–53.
- Freeman GJ, Long AJ, Iwai Y, Bourque K, Chernova T, Nishimura H, et al. Engagement of the PD-1 immunoinhibitory receptor by a novel B7 family member leads to negative regulation of lymphocyte activation. *J Exp Med*. 2000;192(7):1027–34.
- Qin W, Hu L, Zhang X, Jiang S, Li J, Zhang Z, et al. The diverse function of PD-1/PD-L pathway beyond cancer. *Front Immunol*. 2019;10:2298.
- Jayathilake AG, Veale MF, Luwor RB, Nurgali K, Su XQ. Krill oil extract inhibits the migration of human colorectal cancer cells and down-regulates EGFR signalling and PD-L1 expression. *BMC Complement Med Ther*. 2020;20(1):372.
- Das JK, Xiong X, Ren X, Yang J-M, Song J. Heat shock proteins in cancer immunotherapy. *J Oncol*. 2019;2019:3267207.

26. Mosser DD, Caron AW, Bourget L, Denis-Larose C, Massie B. Role of the human heat shock protein hsp70 in protection against stress-induced apoptosis. *Mol Cell Biol*. 1997;17(9):5317–27.
27. Goldstein MG, Li Z. Heat-shock proteins in infection-mediated inflammation-induced tumorigenesis. *J Hematol Oncol*. 2009;2:5.
28. Rohde M, Daugaard M, Jensen MH, Helin K, Nylandsted J, Jaattela M. Members of the heat-shock protein 70 family promote cancer cell growth by distinct mechanisms. *Genes Dev*. 2005;19(5):570–82.
29. Figueiredo C, Wittmann M, Wang D, Dressel R, Seltsam A, Blaszczak R, et al. Heat shock protein 70 (HSP70) induces cytotoxicity of T-helper cells. *Blood*. 2009;113(13):3008–16.
30. Soleimani A, Zahiri E, Ehtiati S, Norouzi M, Rahmani F, Fiuji H, et al. Therapeutic potency of heat-shock protein-70 in the pathogenesis of colorectal cancer: current status and perspectives. *Biochem Cell Biol*. 2019;97(2):85–90.
31. Cai F, Sorg O, Granci V, Lecumberri E, Miralbell R, Dupertuis YM, et al. Interaction of ω -3 polyunsaturated fatty acids with radiation therapy in two different colorectal cancer cell lines. *Clin Nutr*. 2014;33(1):164–70.
32. Chung BH, Mitchell SH, Zhang J-S, Young CYF. Effects of docosahexaenoic acid and eicosapentaenoic acid on androgen-mediated cell growth and gene expression in LNCaP prostate cancer cells. *Carcinogenesis*. 2001;22(8):1201–6.
33. Miller S, Senior PV, Prakash M, Apostolopoulos V, Sakal S, Nurgali K. Leukocyte populations and IL-6 in the tumor microenvironment of an orthotopic colorectal cancer model. *Acta Biochim Biophys Sin*. 2016;48(4):334–41.
34. Munker S, Gerken M, Fest P, Ott C, Schnoy E, Fichtner-Feigl S, et al. Chemotherapy for metastatic colon cancer: no effect on survival when the dose is reduced due to side effects. *BMC Cancer*. 2018;18(1):455.
35. Calviello G, Serini S, Piccioni E, Pessina G. Antineoplastic effects of n-3 polyunsaturated fatty acids in combination with drugs and radiotherapy: preventive and therapeutic strategies. *Nutr Cancer*. 2009;61(3):287–301.
36. Nurgali K, Jagoe RT, Abalo R. Editorial: adverse effects of cancer chemotherapy: anything new to improve tolerance and reduce sequelae? *Front Pharmacol*. 2018;9:245.
37. Vasudevan A, Yu Y, Banerjee S, Woods J, Farhana L, Rajendra SG, et al. Omega-3 fatty acid is a potential preventive agent for recurrent colon cancer. *Cancer Prev Res*. 2014;7(11):138–48.
38. Rani I, Sharma B, Kumar S, Kaur S, Agnihotri N. Apoptosis mediated chemosensitization of tumor cells to 5-fluorouracil on supplementation of fish oil in experimental colon carcinoma. *Tumour Biol*. 2017;39(3):1010428317695019.
39. Barros MP, Poppe SC, Bondan EF. Neuroprotective properties of the marine carotenoid astaxanthin and omega-3 fatty acids, and perspectives for the natural combination of both in krill oil. *Nutrients*. 2014;6(3):1293–317.
40. Biswal S. Oxidative stress and astaxanthin: the novel super nutrient carotenoid. *Int J Health Allied Sci*. 2014;3(3):147–53.
41. Zhang L, Wang H. Multiple mechanisms of anti-cancer effects exerted by astaxanthin. *Mar Drugs*. 2015;13(7):4310–30.
42. Kavitha K, Kowshik J, Kishore TK, Baba AB, Nagini S. Astaxanthin inhibits NF- κ B and Wnt/ β -catenin signaling pathways via inactivation of Erk/MAPK and PI3K/Akt to induce intrinsic apoptosis in a hamster model of oral cancer. *Biochim Biophys Acta*. 2013;1830(10):4433–44.
43. Nagendraprabhu P, Sudhandiran G. Astaxanthin inhibits tumor invasion by decreasing extracellular matrix production and induces apoptosis in experimental rat colon carcinogenesis by modulating the expressions of ERK-2, NF κ B and COX-2. *Invest New Drugs*. 2011;29(2):207–24.
44. Tanaka T, Morishita Y, Suzui M, Kojima T, Okumura A, Mori H. Chemoprevention of mouse urinary bladder carcinogenesis by the naturally occurring carotenoid astaxanthin. *Carcinogenesis*. 1994;15(1):15–9.
45. Zhang X, Zhao WE, Hu L, Zhao L, Huang J. Carotenoids inhibit proliferation and regulate expression of peroxisome proliferators-activated receptor gamma (PPARgamma) in K562 cancer cells. *Arch Biochem Biophys*. 2011;512(1):96–106.
46. Garrido C, Galluzzi L, Brunet M, Puig PE, Didelot C, Kroemer G. Mechanisms of cytochrome c release from mitochondria. *Cell Death Differ*. 2006;13(9):1423–33.
47. Kagan VE, Borisenko GG, Tyurina YY, Tyurin VA, Jiang J, Potapovich AI, et al. Oxidative lipidomics of apoptosis: redox catalytic interactions of cytochrome c with cardiolipin and phosphatidylserine. *Free Radical Biol Med*. 2004;37(12):1963–85.
48. Yan N, Shi Y. Mechanisms of apoptosis through structural biology. *Annu Rev Cell Dev Biol*. 2005;21:35–56.
49. Chai J, Shi Y. Apoptosome and inflammasome: conserved machineries for caspase activation. *Natl Sci Rev*. 2014;1(1):101–18.
50. Klaunig JE, Kamendulis LM, Hocevar BA. Oxidative stress and oxidative damage in carcinogenesis. *Toxicol Pathol*. 2010;38(1):96–109.
51. Alcindor T, Beauger N. Oxaliplatin: a review in the era of molecularly targeted therapy. *Curr Oncol*. 2011;18(1):18–25.
52. Stojanovska V, Sakal S, Nurgali K. Platinum-based chemotherapy: gastrointestinal immunomodulation and enteric nervous system toxicity. *Am J Physiol Gastrointest Liver Physiol*. 2015;308(4):G223–32.
53. Zanardelli M, Micheli L, Nicolai R, Failli P, Ghelardini C, Di Cesare Mannelli L. Different apoptotic pathways activated by oxaliplatin in primary astrocytes vs colo-rectal cancer cells. *Int J Mol Sci*. 2015;16(3):5386–99.
54. Fujie Y, Yamamoto H, Ngan CY, Takagi A, Hayashi T, Suzuki R, et al. Oxaliplatin, a potent inhibitor of survivin, enhances paclitaxel-induced apoptosis and mitotic catastrophe in colon cancer cells. *Jpn J Clin Oncol*. 2005;35(8):453–63.
55. Okada H, Mak TW. Pathways of apoptotic and non-apoptotic death in tumour cells. *Nat Rev Cancer*. 2004;4(8):592–603.
56. Ghiotto M, Gauthier L, Serriari N, Pastor S, Truneh A, Nunes JA, et al. PD-L1 and PD-L2 differ in their molecular mechanisms of interaction with PD-1. *Int Immunol*. 2010;22(8):651–60.
57. Droeser RA, Hirt C, Viehl CT, Frey DM, Nebiker C, Huber X, et al. Clinical impact of programmed cell death ligand 1 expression in colorectal cancer. *Eur J Cancer*. 2013;49(9):2233–42.
58. Dermani FK, Samadi P, Rahmani G, Kohlan AK, Najafi R. PD-1/PD-L1 immune checkpoint: potential target for cancer therapy. *J Cell Physiol*. 2019;234(2):1313–25.
59. Lindquist SL, Kelly JW. Chemical and biological approaches for adapting proteostasis to ameliorate protein misfolding and aggregation diseases: progress and prognosis. *Cold Spring Harb Perspect Biol*. 2011;3(12):004507.
60. Hulina A, Grdic Rajkovic M, Jaksic Despot D, Jelic D, Dojder A, Cepelak I, et al. Extracellular Hsp70 induces inflammation and modulates LPS/LTA-stimulated inflammatory response in THP-1 cells. *Cell Stress Chaperones*. 2018;23(3):373–84.

Publisher's Note

Springer Nature remains neutral with regard to jurisdictional claims in published maps and institutional affiliations.

Ready to submit your research? Choose BMC and benefit from:

- fast, convenient online submission
- thorough peer review by experienced researchers in your field
- rapid publication on acceptance
- support for research data, including large and complex data types
- gold Open Access which fosters wider collaboration and increased citations
- maximum visibility for your research: over 100M website views per year

At BMC, research is always in progress.

Learn more biomedcentral.com/submissions

